of $[Na_2Fe_{18}S_{30}]^{8-}$ (absence of magnetic hyperfine interactions in its Mössbauer spectra), owing to the large separation between rings. This preserves the low magnetic dimensionality nature of the ring, and no long-range magnetic order is expected above absolute zero.[50] For $N \geq 10$ interacting spins $S = {}^1/_2$ in a linear chain (such as are present in some M^1FeS_2 phases), theory predicts that low magnetic dimensionality solid-state effects become evident in magnetic properties.[51,52] Linear magnetic structures such as M^1FeS_2 do not undergo long-range order magnetic phase transitions until the interchain interaction becomes significant enough to drive the system into a three-dimensional magnetic order.[53]

The existence and stability of $[Na_2Fe_{18}S_{30}]^{8-}$ raise a number of questions for further investigation. These include the existence of other cyclic Fe/S structures, removal of the interior Na^+ ions and the stability of $[Fe_{18}S_{30}]^{10-}$, the ability to bind cations other than Na^+ in the cluster interior, and the existence of an analogous (or some other) Fe/Se cluster in which the interior void would be larger and the affinity for Na^+ presumably less.

Acknowledgment. This research was supported by NIH Grant 28856 at Harvard University and by the National Science Foundation at M.I.T. X-ray diffraction equipment was obtained through NIH Grant 1 S10 RR 02247. G.C.P. acknowledges support by the Office of Naval Research program on Cluster Science and Dynamics under Contract No. N00014-89-J-1779. We thank Dr. J. Gao for assistance with the MO calculations.

Supplementary Material Available: Crystallographic data for $(Pr_4N)_6Na_4Fe_{18}S_{30}\cdot 14MeCN$ including tables of data collection parameters, atomic coordinates, thermal parameters, and calculated hydrogen atom positions (7 pages); a table of calculated and observed structure factors (48 pages). Ordering information is given on any current masthead page.

(50) de Jongh, L. J.; Miedema, A. R. *Adv. Phys.* **1974**, *23*, 1.
(51) Bonner, J. C.; Fisher, M. E. *Phys. Rev.* **1964**, *135*, 4640.
(52) des Cloizeaux, J.; Pearson, J. J. *Phys. Rev.* **1962**, *128*, 2131.
(53) Carlin, R. L. *Magnetochemistry*; Springer-Verlag: New York, 1986.

Structural, Spectroscopic, and Chiroptical Properties of the Chiral Quadruple-Bonded Dimolybdenum Complexes $Mo_2Cl_4[(R,R)\text{-DIOP}]_2$ and $Mo_2Cl_4[(S,S)\text{-DIOP}]_2$

Jhy-Der Chen, F. Albert Cotton,* and Larry R. Falvello

Contribution from the Department of Chemistry and Laboratory for Molecular Structure and Bonding, Texas A&M University, College Station, Texas 77843. *Received July 10, 1989*

Abstract: By reaction of $K_4Mo_2Cl_8$ with (*R,R*)- or (*S,S*)-DIOP, (-)- or (+)-2,3-*O*-isopropylidene-2,3-dihydroxy-1,4-bis(diphenylphosphino)butane, two complexes of $Mo_2Cl_4(DIOP)_2$ were prepared. Their UV-vis, CD, and NMR spectra have been recorded, and the crystal structure of $Mo_2Cl_4[(R,R)\text{-DIOP}]_2$ has been determined. Crystal data: space group $P1$, a = 13.406 (8) Å, b = 13.187 (3) Å, c = 11.855 (4) Å, α = 116.34 (2)°, β = 109.69 (3)°, γ = 100.70 (3)°, V = 1623 (3) Å^3, Z = 1. Final residuals: R = 0.0525 and R_w = 0.0728. The structure is disordered so that while only one set of ligand atoms can be resolved, there are two incompletely occupied sets of metal atom positions. In effect there are two different molecules, which have opposite chiralities about the Mo–Mo axis but very similar packing requirements, that randomly occupy the crystal sites. The primary form (P), which is Λ-$Mo_2Cl_4[(R,R)\text{-DIOP}]_2$, occupies 89% of the sites, while the Δ molecules (S) occupy the remaining 11%. The P molecules have a twist angle of −78° and the S molecules an angle of 87°. The ^{1}H NMR spectrum of a solution in CH_2Cl_2 shows that both molecules are again present but now in a P/S ratio of 1.7. Assignment of the various signals to the P and S molecules was possible on an a priori basis because the large diamagnetic anisotropy of the Mo–Mo quadruple bond affects corresponding hydrogen atoms in the two molecules in predictably different ways. An anisotropy of (5700 ± 1200) × 10^{-36} m^3 molecule^{-1} is estimated. The CD spectra of both the *R,R* and *S,S* complexes are found to be fully in accord with the theoretical prediction that a Λ molecule with a twist angle 90° − χ will have the same signs for the CD bands as a Δ molecule with a twist angle χ. The correct absolute sign is predicted in all cases. The UV-vis spectrum is in accord with the twist angle.

Dinuclear, metal–metal-bonded complexes of stoichiometry $M_2X_4(LL)_2$, where LL is a bidentate ligand such as $R_2PCH_2CH_2PR_2$, were first shown by Walton and co-workers[1] to be capable of existing in two isomeric forms, α and β, shown schematically in Figure 1 as a and b. It was soon recognized that the actual structure of the β isomers entails a twist about the metal–metal bond, and many of the electronic, spectroscopic, and structural consequences of this have been investigated in detail.[2,3] One of the most important consequences of the internal twist is that β-$M_2X_4(LL)_2$ molecules are chiral, and this particular phenomenon has been the subject of several previous studies.[4,5] In these investigations it has been shown that there is a simple and rigorous relationship between the direction and magnitude of the internal helicity and the sign of the CD band for the $\delta \rightarrow \delta^*$ transition in those molecules where such a transition is observed.

Another interesting aspect of β-$M_2X_4(LL)_2$ compounds is that generally, though not always, they form crystals in which two conformers that are different (and, importantly, of opposite helicity[6]) occupy each crystallographic site, albeit to different extents.[7] It turns out that these pairs of molecules have very similar arrangements of the ligand atoms in space even though, within a framework approximating to both, the M_2 unit takes one of two different and mutually orthogonal directions. It is the gross outward similarity of the two ligand arrangements that permits the disordered packing of the two types of molecule in the same crystal. However, since the two molecules are merely similar but not identical, even as seen from the outside by their neighbors, they are present in different amounts, one being the P (principal

(1) Ebner, J. R.; Tyler, D. R.; Walton, R. A. *Inorg. Chem.* **1976**, *15*, 833.
(2) Campbell, F. L., III; Cotton, F. A.; Powell, G. L. *Inorg. Chem.* **1985**, *24*, 177.
(3) Campbell, F. L., III; Cotton, F. A.; Powell, G. L. *Inorg. Chem.* **1985**, *24*, 4384.
(4) Agaskar, P. A.; Cotton, F. A.; Fraser, I. F.; Manojlovic-Muir, L.; Muir, K. W.; Peacock, R. D. *Inorg. Chem.* **1986**, *25*, 2511.
(5) Peacock, R. D. *Polyhedron* **1987**, *6*, 715.
(6) Agaskar, P. A.; Cotton, F. A. *Inorg. Chem.* **1984**, *23*, 3383.
(7) Brencic, J. V.; Cotton, F. A. *Inorg. Chem.* **1970**, *9*, 351.

0002-7863/90/1512-1076$02.50/0

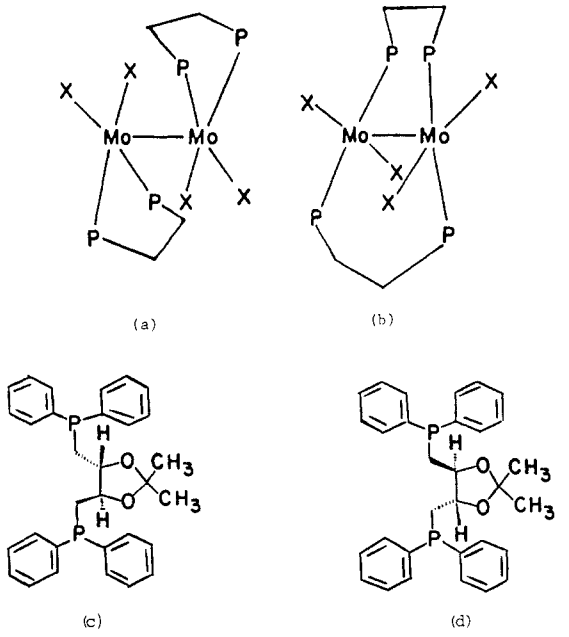

Figure 1. Schematic drawings of structures important in this work: (a and b) the α and β isomers of an $Mo_2X_4(P-P)_2$ compound; (c and d) the *R,R* and *S,S* enantiomorphs of the DIOP ligand.

or predominant) molecule and the other being the S (secondary) molecule.

In spite of our rather extensive knowledge of these systems, as just briefly summarized, several important questions have remained and are not easy to answer. One of these has to do with the prevalence of the P and S forms when the $M_2X_4(LL)_2$ compound is in solution. Presumably the P/S ratio found in the crystal need not remain the same when the substance goes into solution. It is even possible (though perhaps unlikely) that from $P/S > 1$ in the crystal, we could go to $P/S < 1$ in solution. It is also possible that, even when $S/P = 0$ in the crystal (i.e., no secondary form is detectable crystallographically), a nonzero S/P ratio may prevail in solution.

Another question concerns the prediction[4] previously made concerning the relation between the sign of the CD spectrum and the absolute chirality of the β-$M_2X_4(LL)_2$ molecule. The theory requires that a right-hand twist of $45° < \chi < 90°$ give a sign in the CD spectrum equal but opposite to that given by a twist of $0 < \chi < 45°$, where χ is the mean dihedral angle of rotation away from an eclipsed structure. While there is no reason to doubt that this prediction is reliable, the fact is it has never been verified experimentally.

Finally, one more point, allied to the first one, needs to be noted explicitly. If the solution (where the CD is measured) consists of both P and S molecules, which have opposite but similar twist angles, the CD sign and magnitude arise from the difference between P and S contributions, and unless we know the P/S ratio in solution, we cannot develop any quantitative relationship between CD strength and degree of helicity of the molecule.

In an effort to address some or all of these questions, we have prepared and studied the compound $Mo_2Cl_4(DIOP)_2$ where DIOP is the conventional abbreviation for the chiral bis(phosphine) shown in Figure 1 as c and d, the *R,R* and *S,S* forms, respectively. It has turned out that the choice of this bis(phosphine) was a fortunate one, since it has given a great deal of information on all of the above questions.

Experimental Section

General Procedures. All manipulations were carried out under an atmosphere of dry, oxygen-free argon with the Schlenk technique, unless otherwise noted. Solvents were dried and deoxygenated by refluxing over the appropriate reagents before use. Methanol was purified by distillation from magnesium, *n*-hexane from sodium–potassium/benzophenone, and dichloromethane from P_2O_5.

Starting Materials. $K_4Mo_2Cl_8$ was prepared according to a previously reported[7] procedure. The ligands (−)-2,3-*O*-isopropylidene-2,3-dihydroxy-1,4-bis(diphenylphosphino)butane, (*R,R*)-DIOP, and (+)-2,3-*O*-isopropylidene-2,3-dihydroxy-1,4-bis(diphenylphosphino)butane, (*S,S*)-DIOP, were purchased from Strem Chemicals, Inc.

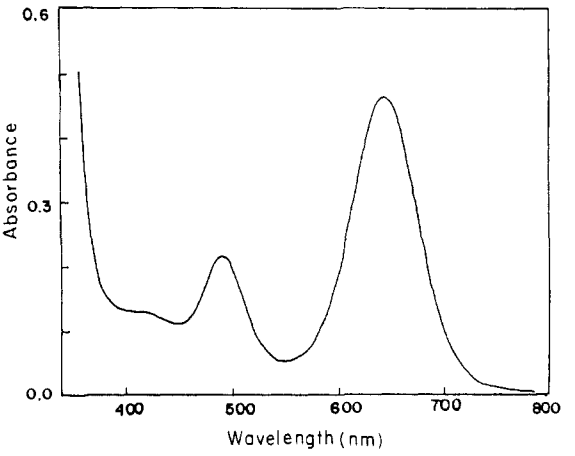

Figure 2. Electronic absorption spectrum of $Mo_2Cl_4[(R,R)\text{-DIOP}]_2$ measured in CH_2Cl_2.

Preparation. $K_4Mo_2Cl_8$ (0.10 g, 0.16 mmol) and (*R,R*)-DIOP (0.16 g, 0.32 mmol), or the same amount of (*S,S*)-DIOP, were placed in a flask equipped with a reflux condenser. Methanol (6 mL) was then added. This mixture was refluxed for 6 h to yield a green solution and green solid. The solid was filtered off, washed with methanol and ether, and then dried under vacuum; yield 0.10 g (47%) for $Mo_2Cl_4[(R,R)\text{-DIOP}]_2$ or 0.08 g (38%) for $Mo_2Cl_4[(S,S)\text{-DIOP}]_2$. Solutions of these two complexes were found to be air-sensitive, but the solids were air-stable.

The visible absorption spectrum of $Mo_2Cl_4[(R,R)\text{-DIOP}]_2$ in dichloromethane had bands at 645 and 490 nm and a shoulder at 420 nm. This spectrum, obtained with a Cary 14 spectrophotometer, is shown in Figure 2. ^1H NMR spectra were obtained on a Varian XL 200 NMR spectrometer, operating in the Fourier transform mode at room temperature. CD_2Cl_2 was used as the solvent. The spectrum of $Mo_2Cl_4[(R,R)\text{-DIOP}]_2$ is shown in Figure 3. The circular dichroism (CD) spectra were obtained on a Cary 60 spectrophotometer. The CD spectra of $Mo_2Cl_4[(R,R)\text{-DIOP}]_2$ and $Mo_2Cl_4[(S,S)\text{-DIOP}]_2$ are mirror images, within experimental error, as shown in Figure 4.

X-ray Diffraction Procedure. Crystals suitable for X-ray diffraction measurement were obtained by hexane-induced crystallization from a dichloromethane solution. A green crystal was mounted with epoxy cement on a glass fiber. Routine 2θ–ω data collection was carried out at room temperature (20 ± 1°) with use of an Enraf-Nonius CAD-4 diffractometer equipped with Mo Kα graphite-monochromated X-radiation. Three check reflections monitored throughout the data collection displayed no significant gain or loss in intensity.

The data were processed and the structure was solved and refined by employing the Enraf-Nonius SDP and SHELX 76 software packages on a VAX computer. Empirical absorption corrections based on azimuthal (ψ) scans of reflections with Eulerian angle χ near 90° were applied to the data.

Structure Solution. The unit cell constants were determined from 24 reflections with 2θ values in the range from 21 to 32°. These were consistent with a triclinic crystal system and with 1 chiral molecule per cell. The space group was initially assumed, and subsequently shown, to be *P*1.

The Mo atoms were located in a Patterson map, and the remaining atoms were found in a series of difference Fourier maps alternating with least-squares refinement of the atoms found. Anisotropic thermal parameters were used for all the atoms except hydrogen atoms. The refinement, which was conducted with the program SHELX76, was blocked. Although the total number of variables was 654, no more than 450 parameters were refined in a given cycle.

The structure as initially solved appeared to contain the wrong enantiomorph of the ligand (i.e., *S,S* instead of *R,R*). An inversion of coordinates was made, and then both structures were refined to convergence. The results clearly confirmed that the *R,R* isomer was indeed correct. For *R* and R_w, the *R,R* isomer gave 0.0525 and 0.0728, respectively, while the corresponding figures for the *S,S* case were 0.0529 and 0.0735. It is noteworthy that the absolute chirality of the DIOP ligand has been established previously by anomalous dispersion.[8] In a study of the platinum complex $PtCl(CH_3)[(+)\text{-DIOP}]$, it was shown that the (+)-DIOP has the *S,S* chirality. The correct *S,S* and incorrect *R,R*

(8) Payne, N. C.; Stephan, D. W. *J. Organomet. Chem.* **1982**, *228*, 203.

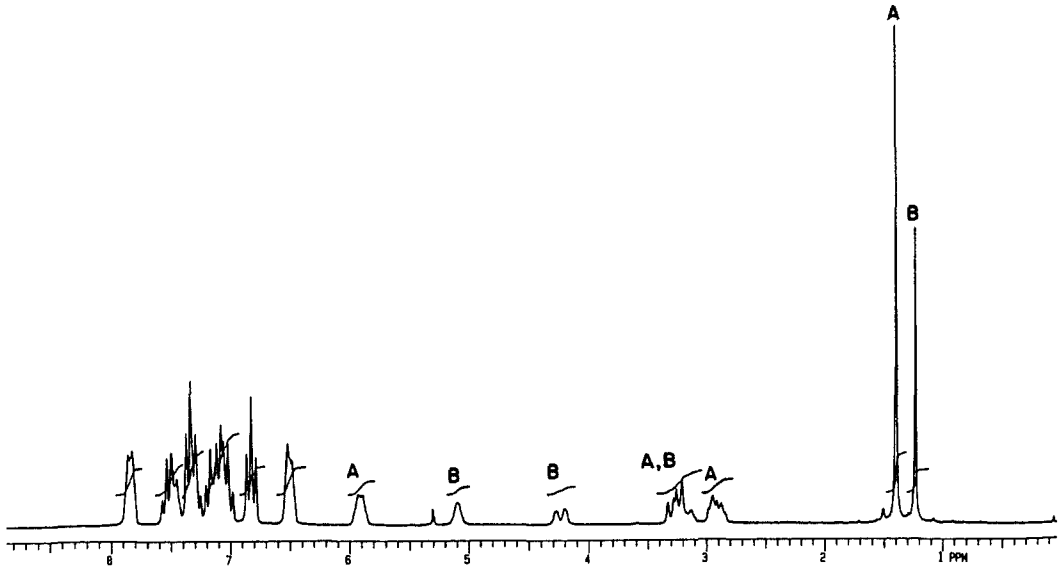

Figure 3. ^{1}H NMR spectrum of $Mo_2Cl_4[(R,R)\text{-DIOP}]_2$ measured in CD_2Cl_2 at 200 MHz.

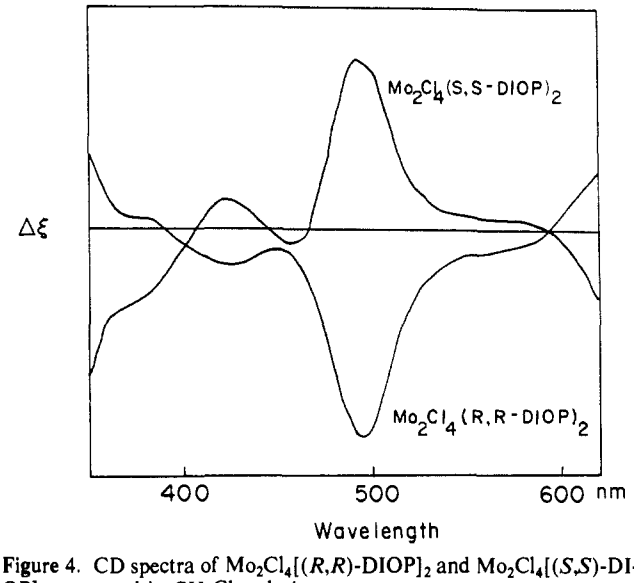

Figure 4. CD spectra of $Mo_2Cl_4[(R,R)\text{-DIOP}]_2$ and $Mo_2Cl_4[(S,S)\text{-DIOP}]_2$ measured in CH_2Cl_2 solution.

enantiomers in this case gave R and R_w values of 0.0668 and 0.0630 vs 0.0699 and 0.0673.

Parameters pertaining to data collection and refinement are listed in Table I. Final atomic positions and anisotropic thermal parameters are listed in Table II. Selected bond distances and angles are listed in Table III.

Results and Discussion

Crystal Structure. The X-ray crystal structure shows two different molecules, which have different chiralities, partially occupying a given site. Figure 5 illustrates the complete molecular geometry and gives the atom labeling scheme for the principal and secondary forms of the complex $Mo_2Cl_4[(R,R)\text{-DIOP}]_2$. The principal molecule has a counterclockwise or left-hand helicity (Λ), while the secondary molecule has a clockwise or right-hand helicity (Δ). At each crystallographic site the percentage of the P form is 89 and the S form 11, so that the ratio, P/S, in the crystal is 8.1. The torsional angles, χ, of the P and S forms are found to be −78° and 87°, respectively. In each form, eight-membered rings are formed by two molybdenum, two phosphorus, and four carbon atoms. The conformations of these eight-membered rings can also be designated as λ and δ, if the center of the Mo–Mo bond is supposed to occupy the position of the single metal atom in a mononuclear chelate complex, just as the case in the seven-membered ring. It will be seen that these rings have a λ conformation in both P and S forms. It is to be noted that the conformations of the segments of Mo–P–C–C and P–C–C–C are also λ.

Table I. Crystal Data for $Mo_2Cl_4[(R,R)\text{-DIOP}]_2\cdot 0.75CH_2Cl_2$

formula	$Mo_2Cl_4P_4O_4C_{62}H_{64}\cdot 0.75CH_2Cl_2$
formula weight	1394.45
space group	$P1$
a, Å	13.406 (8)
b, Å	13.187 (3)
c, Å	11.855 (4)
α, deg	116.34 (2)
β, deg	109.69 (3)
γ, deg	100.70 (3)
V, Å^3	1623 (3)
Z	1
d_{calc}, g/cm^3	1.43
cryst size, mm	0.39 × 0.26 × 0.13
μ(Mo Kα), cm^{-1}	7.50
data collectn instrument	Enraf-Nonius CAD-4
radiat monochrom in incident beam (λ(Mo Kα), Å)	0.71073
orientation reflcns: no., range (2θ)	24, 21.1 < $2\theta \leq$ 31.6
temp, °C	20 ± 1
scan method	2θ–ω
data collectn range (2θ), deg	$4 \leq 2\theta \leq 50$
no. unique data, total no. with $F_o^2 > 3\sigma(F_o^2)$	5953, 5380
no. param refined	654 (see text)
transmissn factors: max, min	1.00, 0.88
R^a	0.0525
$R_w{}^b$	0.0728
quality-of-fit indicator^c	1.758
largest shift/esd, final cycle	0.73
largest peak, e/Å^3	0.90

$^a R = \sum||F_o| - |F_c||/\sum|F_o|$. $^b R_w = [\sum w(|F_o| - |F_c|)^2/\sum w|F_o|^2]^{1/2}$; $w = 1/\sigma^2(|F_o|)$. ^{c}Quality-of-fit = $[\sum w(|F_o| - |F_c|)^2/(N_{obsd} - N_{param})]^{1/2}$.

NMR Spectra. As shown in Figure 3, the ^{1}H NMR spectrum displays two sets of peaks with different intensities, which can be assigned to two different complexes. We may reasonably assume that these correspond to the P form and S form in the solid-state crystal structure, but it remains to be determined which is which. Therefore, we shall begin by calling one of the two complexes in solution A and the other B.

The peaks were well separated except for the multiplet at 3.1–3.4 ppm, which is a combination of two resonances, one from each of the two complexes. The peaks at 1.4, 2.9, and 5.9 ppm and one of the peaks in the mixed multiplet have higher intensities than the other set; these were assigned to complex A. The weaker set, namely peaks at 1.2, 4.15–4.25, and 5.1 ppm, and one of the peaks of the multiplet were assigned to complex B. Table IV lists the chemical shifts of free DIOP, complex A (which turns out

Table II. Positional and Isotropic Equivalent Thermal Parameters (Å^2) and Their Estimated Standard Deviations for $Mo_2Cl_4[(R,R)\text{-DIOP}]_2\cdot 0.75CH_2Cl_2$

atom	*x*	*y*	*z*	B^a (Å^2)	atom	*x*	*y*	*z*	B^a (Å^2)
Mo(1)	−0.225	−0.756	−0.169	2.20 (3)	C(29)	−0.7263 (8)	−1.3068 (8)	−0.3484 (9)	8 (1)
Mo(2)	−0.325 58 (8)	−0.927 23 (8)	−0.2098 (1)	2.28 (3)	C(30)	−0.7250 (8)	−1.3172 (8)	−0.4702 (9)	7.9 (9)
Mo(1′)	−0.2355 (8)	−0.8889 (7)	−0.2395 (7)	3.1 (3)	C(31)	−0.6714 (8)	−1.2122 (8)	−0.4641 (9)	6.1 (6)
Mo(2′)	−0.3137 (7)	−0.7961 (7)	−0.1205 (7)	2.9 (3)	C(32)	−0.0208 (9)	−0.5964 (9)	0.243 (1)	3.7 (3)
Cl(1)	−0.3463 (2)	−0.6447 (2)	−0.1900 (3)	3.60 (9)	C(33)	−0.030 (1)	−0.711 (1)	0.249 (1)	3.8 (4)
Cl(2)	−0.3846 (2)	−1.0928 (2)	−0.4489 (3)	3.71 (9)	C(34)	−0.0012 (9)	−0.804 (1)	0.143 (1)	3.2 (4)
Cl(3)	−0.3339 (3)	−0.8878 (3)	0.0063 (3)	4.0 (1)	C(35)	−0.0834 (9)	−0.9399 (9)	0.062 (1)	3.5 (4)
Cl(4)	−0.0296 (2)	−0.7383 (3)	−0.1162 (3)	3.53 (9)	O(3)	0.060 (1)	−0.665 (1)	0.3865 (9)	7.2 (5)
P(1)	−0.2485 (2)	−0.7961 (3)	−0.4140 (3)	2.72 (8)	O(4)	0.1138 (6)	−0.7824 (7)	0.2336 (7)	3.7 (3)
P(2)	−0.5420 (2)	−0.9572 (3)	−0.3211 (3)	3.17 (9)	C(36)	0.129 (1)	−0.735 (1)	0.377 (1)	4.1 (4)
P(3)	−0.1395 (2)	−0.5952 (2)	0.1056 (3)	2.87 (8)	C(37)	0.090 (1)	−0.838 (1)	0.396 (1)	5.8 (6)
P(4)	−0.1811 (2)	−1.0181 (2)	−0.1307 (3)	2.84 (9)	C(38)	0.251 (1)	−0.650 (1)	0.480 (2)	7.4 (6)
C(1)	−0.3845 (8)	−0.8007 (9)	−0.528 (1)	3.3 (4)	C(39)	−0.2323 (7)	−0.5507 (7)	0.1876 (8)	3.4 (3)
C(2)	−0.4869 (8)	−0.919 (1)	−0.594 (1)	3.3 (4)	C(40)	−0.2485 (7)	−0.5890 (7)	0.2748 (8)	4.5 (4)
C(3)	−0.5739 (9)	−0.904 (1)	−0.536 (1)	3.3 (4)	C(41)	−0.3133 (7)	−0.5479 (7)	0.3422 (8)	5.6 (5)
C(4)	−0.6122 (8)	−1.002 (1)	−0.507 (1)	3.8 (4)	C(42)	−0.3619 (7)	−0.4685 (7)	0.3224 (8)	6.0 (5)
O(1)	−0.5583 (6)	−0.9730 (8)	−0.7446 (8)	4.1 (3)	C(43)	−0.3458 (7)	−0.4302 (7)	0.2351 (8)	5.7 (6)
O(2)	−0.6713 (8)	−0.918 (1)	−0.649 (1)	5.9 (5)	C(44)	−0.2809 (7)	−0.4713 (7)	0.1677 (8)	4.3 (4)
C(5)	−0.651 (1)	−0.937 (1)	−0.762 (1)	4.5 (5)	C(45)	−0.0555 (7)	−0.4457 (6)	0.1426 (6)	3.3 (3)
C(6)	−0.628 (2)	−0.827 (2)	−0.773 (2)	8 (1)	C(46)	−0.0119 (7)	−0.3405 (6)	0.2787 (6)	4.8 (4)
C(7)	−0.761 (1)	−1.049 (2)	−0.900 (2)	8.0 (8)	C(47)	0.0502 (7)	−0.2256 (6)	0.3105 (6)	5.1 (4)
C(8)	−0.2261 (7)	−0.9193 (7)	−0.5418 (6)	3.2 (3)	C(48)	0.0685 (7)	−0.2158 (6)	0.2060 (6)	4.8 (4)
C(9)	−0.1594 (7)	−0.9755 (7)	−0.4941 (6)	4.7 (5)	C(49)	0.0249 (7)	−0.3209 (6)	0.0699 (6)	4.9 (5)
C(10)	−0.1410 (7)	−1.0697 (7)	−0.5900 (6)	6.1 (7)	C(50)	−0.0371 (7)	−0.4358 (6)	0.0382 (6)	4.0 (4)
C(11)	−0.1894 (7)	−1.1078 (7)	−0.7335 (6)	5.4 (5)	C(51)	−0.0910 (4)	−1.0658 (6)	−0.2156 (6)	3.1 (3)
C(12)	−0.2561 (7)	−1.0516 (7)	−0.7812 (6)	5.4 (5)	C(52)	−0.1423 (4)	−1.1791 (6)	−0.3459 (6)	4.1 (4)
C(13)	−0.2745 (7)	−0.9574 (7)	−0.6854 (6)	4.2 (4)	C(53)	−0.0754 (4)	−1.2228 (6)	−0.4083 (6)	4.3 (4)
C(14)	−0.1429 (6)	−0.6551 (6)	−0.367 (1)	3.6 (4)	C(54)	0.0428 (4)	−1.1533 (6)	−0.3404 (6)	4.5 (5)
C(15)	−0.0352 (6)	−0.6498 (6)	−0.357 (1)	5.0 (5)	C(55)	0.0941 (4)	−1.0400 (6)	−0.2101 (6)	4.4 (4)
C(16)	0.0454 (6)	−0.5418 (6)	−0.321 (1)	7.3 (8)	C(56)	0.0272 (4)	−0.9963 (6)	−0.1477 (6)	4.1 (4)
C(17)	0.0182 (6)	−0.4391 (6)	−0.294 (1)	5.5 (5)	C(57)	−0.2663 (6)	−1.1652 (7)	−0.164 (1)	3.3 (4)
C(18)	−0.0895 (6)	−0.4444 (6)	−0.303 (1)	5.0 (5)	C(58)	−0.3866 (6)	−1.2161 (7)	−0.239 (1)	5.7 (6)
C(19)	−0.1700 (6)	−0.5525 (6)	−0.340 (1)	4.6 (5)	C(59)	−0.4491 (6)	−1.3273 (7)	−0.263 (1)	7.3 (8)
C(20)	−0.6076 (5)	−0.8553 (9)	−0.2387 (7)	3.4 (4)	C(60)	−0.3912 (6)	−1.3876 (7)	−0.212 (1)	6.4 (7)
C(21)	−0.5472 (5)	−0.7640 (9)	−0.0927 (7)	6.5 (5)	C(61)	−0.2709 (6)	−1.3366 (7)	−0.136 (1)	5.1 (5)
C(22)	−0.6017 (5)	−0.6962 (9)	−0.0270 (7)	8.6 (7)	C(62)	−0.2084 (6)	−1.2254 (7)	−0.112 (1)	4.3 (4)
C(23)	−0.7165 (5)	−0.7198 (9)	−0.1072 (7)	7.6 (8)	C(63)	−0.5550	−0.2559	0.1440	8
C(24)	−0.7770 (5)	−0.8111 (9)	−0.2532 (7)	6.8 (7)	Cl(5)	−0.5608	−0.3548	−0.0226	14
C(25)	−0.7225 (5)	−0.8788 (9)	−0.3190 (7)	6.2 (6)	Cl(6)	−0.6722	−0.3338	0.1551	21
C(26)	−0.6191 (8)	−1.0968 (8)	−0.3362 (9)	4.7 (5)	C(64)	−0.7591	−0.4321	0.1700	28
C(27)	−0.6204 (8)	−1.0864 (8)	−0.2144 (9)	5.8 (7)	Cl(7)	−0.6595	−0.3689	0.1257	28
C(28)	−0.6740 (8)	−1.1914 (8)	−0.2205 (9)	8 (1)	Cl(8)	−0.7073	−0.5209	0.2352	28

[a] Anisotropically refined atoms are given in the form of the equivalent isotropic displacement parameter defined as $^4/_3[a^2\beta_{11} + b^2\beta_{22} + c^2\beta_{33} + ab(\cos\gamma)\beta_{12} + ac(\cos\beta)\beta_{13} + bc(\cos\alpha)\beta_{23}]$.

Table III. Selected Bond Distances (Å) and Angles (deg) for $Mo_2Cl_4[(R,R)\text{-DIOP}]_2\cdot 0.75CH_2Cl_2$[a]

Distances

Mo(1)-Mo(2)	2.149 (1)	Mo(1′)-Cl(2)	2.475 (6)	Mo(2)-P(4)	2.589 (4)	Mo(2)-Cl(3)	2.425 (4)
Mo(2′)-P(3)	2.616 (6)	Mo(1′)-P(4)	2.622 (11)	Mo(1′)-Cl(4)	2.524 (9)	Mo(1′)-Mo(2′)	2.127 (14)
Mo(1)-P(3)	2.623 (2)	Mo(2′)-P(2)	2.781 (7)	Mo(2′)-Cl(1)	2.528 (11)	Mo(1′)-P(1)	2.810 (11)
Mo(2)-P(2)	2.617 (3)	Mo(1)-Cl(4)	2.417 (3)	Mo(1)-Cl(1)	2.407 (3)	Mo(2′)-Cl(3)	2.359 (11)
		Mo(2)-Cl(2)	2.405 (3)	Mo(1)-P(1)	2.598 (3)		

Angles

Cl(4)-Mo(1′)-P(1)	78.6 (3)	Mo(2)-P(4)-C(51)	123.6 (3)	Cl(4)-Mo(1′)-P(4)	94.1 (3)
Mo(2)-Mo(1)-Cl(1)	108.29 (8)	P(1)-Mo(1′)-P(4)	157.0 (4)	Cl(1)-Mo(2′)-Cl(3)	149.9 (5)
Mo(2)-Mo(1)-Cl(4)	110.44 (9)	Cl(4)-Mo(1)-P(1)	84.8 (1)	Mo(2)-Mo(1)-P(1)	107.09 (7)
Mo(2)-Mo(1)-P(3)	105.46 (8)	Mo(1′)-Mo(2′)-P(3)	103.3 (4)	Cl(1)-Mo(1)-P(3)	83.03 (9)
Mo(1′)-Mo(2′)-Cl(1)	104.5 (5)	Cl(1)-Mo(1)-Cl(4)	141.3 (1)	Mo(1′)-Mo(2′)-Cl(3)	105.6 (5)
Cl(1)-Mo(1)-P(1)	84.6 (1)	Mo(1′)-Mo(2′)-P(2)	97.5 (3)	Cl(4)-Mo(1)-P(3)	86.18 (9)
Cl(1)-Mo(2′)-P(2)	88.8 (3)	P(1)-Mo(1)-P(3)	147.4 (1)	Cl(1)-Mo(2′)-P(3)	80.9 (3)
Cl(3)-Mo(2′)-P(2)	85.6 (3)	Cl(3)-Mo(2′)-P(3)	93.9 (3)	Cl(2)-Mo(2)-Cl(3)	141.5 (1)
Mo(1)-Mo(2)-Cl(2)	109.9 (1)	P(2)-Mo(2′)-P(3)	158.5 (4)	Mo(1)-Mo(2)-Cl(3)	108.51 (8)
Mo(1)-Mo(2)-P(2)	107.04 (9)	Mo(1)-Mo(2)-P(4)	106.49 (7)	Cl(2)-Mo(2)-P(2)	83.0 (1)
Cl(2)-Mo(2)-P(4)	85.1 (1)	Cl(3)-Mo(2)-P(2)	88.0 (1)	Cl(3)-Mo(2)-P(4)	82.1 (1)
P(2)-Mo(2)-P(4)	146.5 (1)	Cl(2)-Mo(1′)-P(4)	83.0 (3)	Mo(2′)-Mo(1′)-P(4)	100.9 (5)
Cl(2)-Mo(1′)-Cl(4)	145.5 (5)	Cl(2)-Mo(1′)-P(1)	90.8 (3)		

[a] Numbers in parentheses are estimated standard deviations in the least significant digits.

to be Λ-$Mo_2Cl_4[(R,R)\text{-DIOP}]_2$), and complex B (which turns out to be Δ-$Mo_2Cl_4[(R,R)\text{-DIOP}]_2$).

The procedure by which we were able to associate the stronger set of signals, those for complex A, with the crystallographic principal isomer P and identify complex B in solution with the crystallographic secondary isomer, S, will now be explained.

(1) We first noted that the A and B spectra, as well as the spectrum of the free ligand, fall into three regions. From 6.6 to 8.0 ppm we have the aromatic protons. These are of no use for our analysis and will not be discussed further. In the region 1.0–1.5

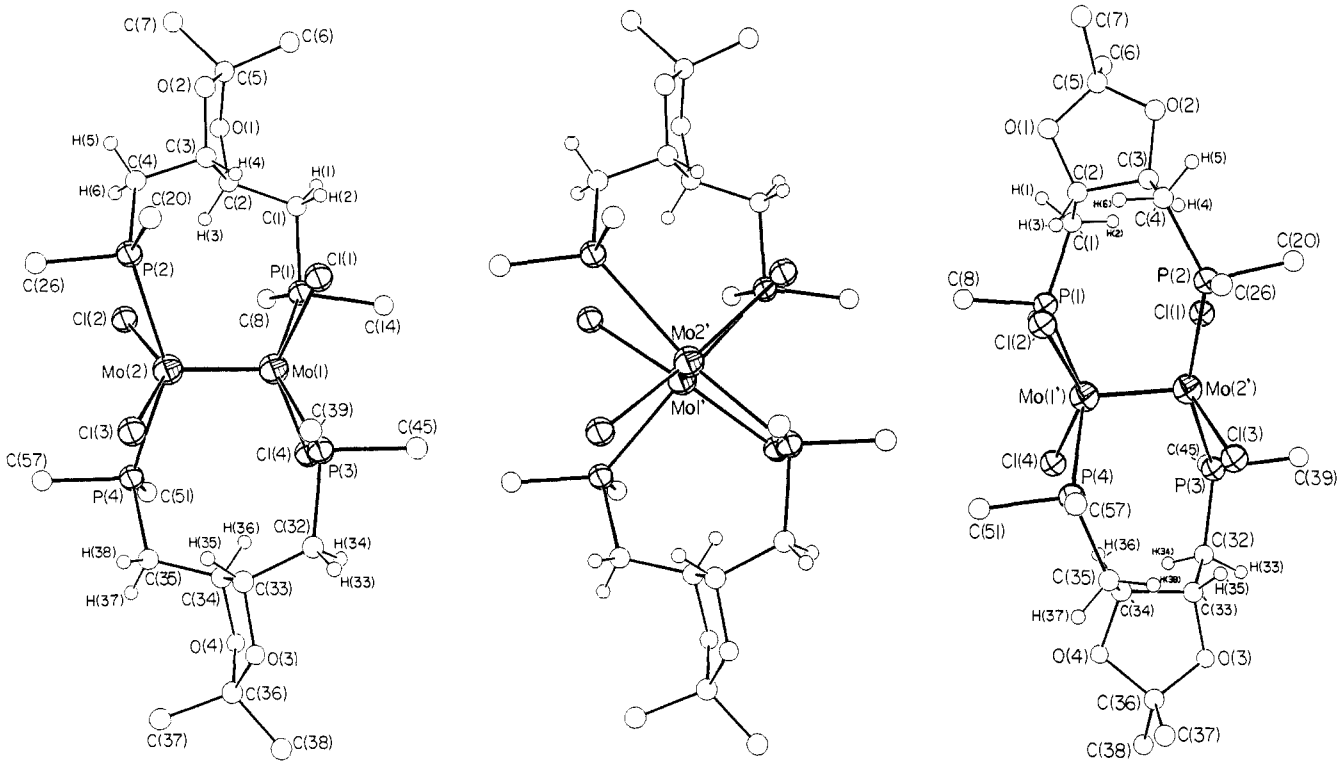

Figure 5. Three ORTEP drawings showing the molecular structures of the two isomers of $Mo_2Cl_4[(R,R)\text{-DIOP}]_2$: left, the principal (P) isomer in the crystal; center, the secondary (S) isomer, with the ligands viewed exactly as for the P isomer; right, the secondary isomer turned to give a side view of the Mo–Mo unit.

Table IV. ^1H NMR Chemical Shifts[a] for DIOP and the Two $Mo_2Cl_4(DIOP)_2$ Complexes A and B

	aromatic	CH	CH_2	CH_3
DIOP	7.2–7.6	3.89	2.33	1.30
complex A	6.6–8.0	5.92	2.92, 3.25	1.39
complex B		5.12	4.23, 3.20	1.23

[a] In ppm downfield from TMS as 0.0, measured in CD_2Cl_2.

ppm we have the methyl signals. On the basis that for each isomer the symmetry is D_2, there should be only one methyl signal for each. Thus, the two observed signals tell us that two (and only two) isomers are present in detectable amounts and give us a fairly accurate ratio of their concentrations, namely, 1.7 for A/B. The assumption of D_2 symmetry with equivalence of the two methyl groups in each geminal pair entails the assumption that the five-membered rings are conformationally flexible and flipping rapidly.

(2) We are now left with the spectral region 2.0–6.0 ppm, in which we find signals for the bridgehead (C–H) and methylene (CH_2) protons. The key observation is that in the complexes chemical shifts for these are spread over a wide range. The reason for this spread is qualitatively easy to see when the two structures are examined. These hydrogen atoms are positioned very differently with respect to the Mo_2 unit in the P and S isomers. Since the quadruple bond in Mo_2^{4+} has been shown to have an enormous diamagnetic anisotropy,[9] it strongly affects the chemical shifts of all nearby hydrogen atoms and can cause large differences between those that lie in different regions of space.

To illustrate this point, consider the CH hydrogen atoms in the P and S isomers. By inspection of Figure 5, it is clear that in both cases these methine hydrogen atoms are about the same distance, r, from the midpoint of the Mo_2 unit but that they lie along vectors from the midpoint that make quite different angles, θ, with the Mo–Mo axis. These important parameters, r and θ, are defined in Figure 6. According to the well-known physical picture of how an anisotropic, axially symmetric entity (such as Mo$\overset{4}{-}$Mo) affects

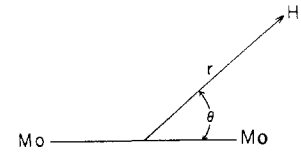

Figure 6. Diagram showing how the vector r and the angle θ are defined.

protons near it, those that lie right over the midpoint (i.e., those with $\theta = 90°$) will be shifted maximally downfield, while those that have smaller θ angles will be shifted less (and eventually, for θ angles less than $\cos^{-1}\theta = 1/\sqrt{3}$, upfield). Actual calculations for the P and S structures show that for CH protons in the P isomer $\theta = 84.5°$ and in the S isomer $\theta = 71.0°$. Thus, we can associate the most downfield methine proton signal (that in spectrum A) with the P isomer and the other one (spectrum B) with the S isomer.

Since the two CH signals at ca. 5.9 and 5.1 ppm are in an intensity ratio of 1.7, we thus learn that the P isomer is also the major isomer in solution but only by a ratio of 1.7 rather than the ratio of 8.9 that prevailed in the crystal. That a difference exists is, of course, not surprising, as anticipated in the introduction, since the solution and crystal environments are quite different and should therefore affect the relative stabilities of the two molecules differently.

(3) We next extend the preceding argument, which was applied only to the CH protons, and employed only qualitatively, to deal quantitatively with the entire CH and CH_2 region of the spectrum. To do this, we employ the equation that relates diamagnetic anisotropy, $\Delta\chi$ ($=\chi_\parallel - \chi_\perp$), to the chemical shifts and geometric factors, r and θ, namely

$$\Delta\delta = \Delta\chi[(1 - 3\cos^2\theta)/12\pi r^3] = \Delta\chi G$$

From the structural data we calculate the geometric factors, G, for the CH, proximal CH_2 (CH_2^p), and distal CH_2(CH_2^d) protons of each isomer. The details of these calculations are available in the supplementary material. Only the G factors themselves are given here in Table V. From the NMR spectra we calculate the change in chemical shift, $\Delta\delta$, for each type of proton in each isomer from the chemical shift it has in the uncoordinated ligand.

(9) Cotton, F. A.; Kitagawa, S. *Polyhedron* **1988**, *7*, 1673.

Table V. Changes in Chemical Shifts ($\Delta\delta$) and Geometric Factors for the Two Isomers of $Mo_2Cl_4[(R,R)\text{-DIOP})]_2$

	type of proton[a]		
	CH	CH_2^p	CH_2^d
$\Delta\delta$ (ppm) in A spectrum	2.03	0.92	0.59
G (m^{-3}) × 10^{-26} in P isomer	4.68	1.07	0.91
$\Delta\delta$ (ppm) in B spectrum	1.23	1.90	0.87
G (m^{-3}) × 10^{-26} in S isomer	3.27	3.37	1.45

[a] Superscripts p and d denote proximal and distal.

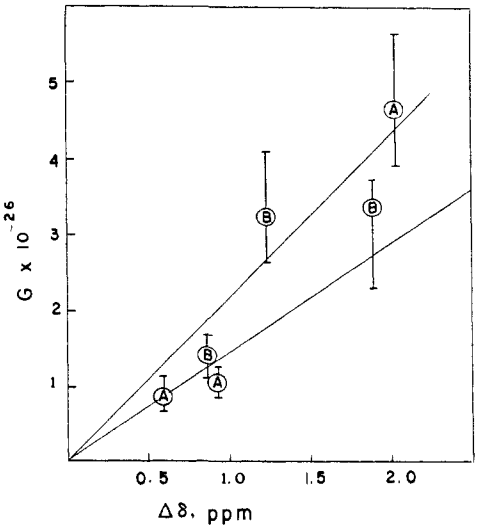

Figure 7. Plot of G vs $\Delta\delta$ (ppm) (see Table V). The two lines are discussed in the text.

These results are also given in Table V.

If our model were perfect, a plot of the $\Delta\delta$ vs G would give a straight line passing through the origin, with a slope of $1/\Delta\chi$. Such a plot is shown in Figure 7. Clearly, our model is not perfect, but it is not bad. The best line passing through the two points for the CH protons gives $\Delta\chi = 4500 \times 10^{-36}$ m^3 while the best line passing through the four points for CH_2 protons gives $\chi = 6900 \times 10^{-36}$ m^3. These two values bracket the average value of ca. 6500×10^{-36} m^3 previously found[9] for the Mo–Mo quadruple bond in related compounds.

We have said that the scatter of points in Figure 7 shows that our model is imperfect. There are several reasons why this is so. One, which is perhaps least obvious, but real and inescapable, is that the structures used to calculate the G terms are only approximate descriptions of the molecules in solution that give rise to the A and B spectra. Because the ligand atom positions refined for the crystal structure are not actually those for either the P or the S isomer but rather a weighted average of the two, the G terms cannot be exactly suitable as calculated. In addition, the conformations of the P or S (or both) molecules may change somewhat when they pass from the crystal to the solution environment, and for this reason as well the calculated G terms may differ from those that truly apply to the molecules in solution. Neither of these effects is expected to be large, but they could certainly lead to the observed scatter.

In addition to the considerations just mentioned, we must also recognize that the chemical shift differences, $\Delta\delta$, may be influenced, at least slightly, by factors other than the diamagnetic anisotropy of the Mo_2 unit. Among these factors are inductive effects resulting from coordination of the phosphorus atoms to the Mo_2^{4+} entity, hybridization changes at the carbon atoms resulting from changes in bond and torsion angles upon coordination, and altered spatial relationship of the CH and CH_2 protons relative to the magnetically anisotropic phenyl groups. While none of these is expected to be as important as the diamagnetic anisotropy of the Mo_2 entity, at least as far as the close-in protons that we deal with in Figure 7 are concerned, they could certainly cause small deviations from the ideal behavior expected if they were nonexistent.

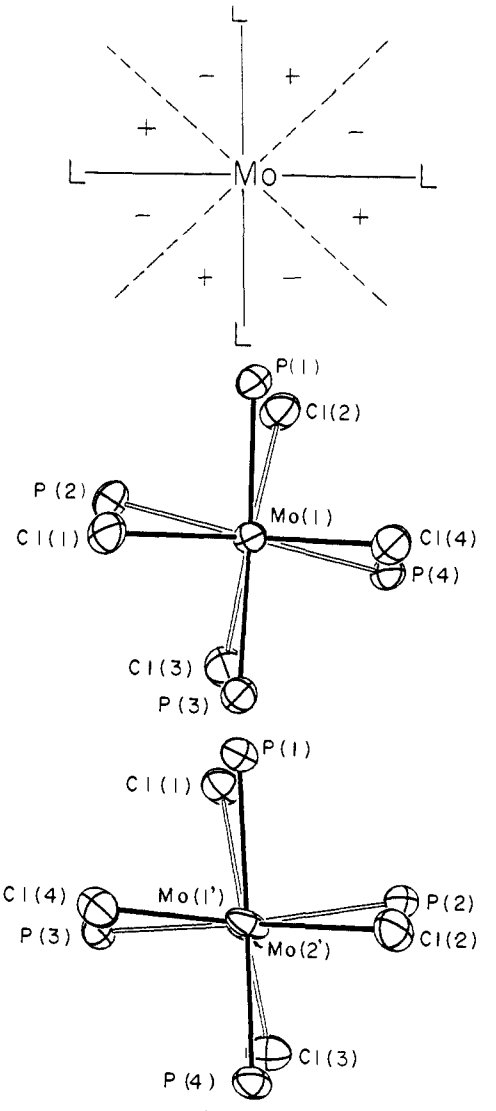

Figure 8. Sector diagram (top) for the $\delta \rightarrow \delta^*$ transition of a chiral $Mo_2L_nL'_{8-n}$ complex and axial views of the $Mo_2Cl_4P_4$ cores of the P (center) and S (lower) isomers of the $Mo_2Cl_4[(R,R)\text{-DIOP}]_2$ molecule.

Before leaving the subject of NMR spectra, we should report that the ^{13}C NMR spectrum was also recorded and assigned, and it fully agrees with the presence of two isomers in a 1.7 ratio. However, there is no way to use internal evidence to decide which spectrum belongs to which isomer in this case, since the $\Delta\delta$ values for ^{13}C resonances depend on a number of factors that are as large or larger than the diamagnetic anisotropy effects that are predominant for the inner protons. For example, the CH_2 carbon atoms in the two isomers have $\Delta\delta$ greater than 8 ppm.

Absorption and CD Spectra. The absorption spectrum (Figure 2) is typical for compounds with Mo–Mo quadruple bonds.[10] The lowest energy band at 645 nm (15 750 cm^{-1}) is due to the $\delta \rightarrow \delta^*$ ($^1A_{1g} \rightarrow {}^1A_{2u}$) transition, and the one at 490 nm is due to a forbidden transition often described as $\delta_{xy} \rightarrow \delta_{x^2-y^2}$. It must be kept in mind that what we are actually seeing is the convolution of the spectra of both the P and S molecules in a P/S ratio of 1.7. However, the twist angles in these two molecules are very similar (±78°, ∓87°), and when we refer to the previously determined relationship[2] between χ and the position of the $\delta \rightarrow \delta^*$ transition, we estimate transition energies of 15 800 and 15 900 cm^{-1} for the P and S forms, respectively. These are so similar that the spectra are virtually superposed, and the observed maximum is in satisfactory agreement with the average, ca. 15 820 cm^{-1}, of the predicted values.

(10) Cotton, F. A.; Walton, R. A. *Multiple Bonds between Metal Atoms*; John Wiley & Sons: New York, 1982; p 390.

Turning now to the CD spectrum, we come to the major objective of this work. It is clear from Figure 4 that there is a mirror-image relationship between the spectra of the enantiomorphic molecules, due allowance being made for a slightly sloping base line. The instrument used to measure these spectra is insensitive beyond about 620 nm, but it is clear that in the range 590–620 nm a CD band lying further to the red is being approached and that this is opposite in sign to the one at 490 nm. This relationship of opposite signs for the $\delta \rightarrow \delta^*$ and $\delta_{xy} \rightarrow \delta_{x^2-y^2}$ CD bands has been observed consistently in the past[5] and is to be expected theoretically.

All previous theorizing about the relationship between the absolute chirality of a twisted $Mo_2L_nL'_{8-n}$ molecule and the sign of the CD band for the $\delta \rightarrow \delta^*$ transition can be summarized in the sector diagram at the top of Figure 8. To apply this diagram, we consider only the two sets of four-coordinated atoms, one set on each metal atom. The diagram shows the upper metal atom and its four ligands. If the lower ML_4 group is rotated so that the M–L bonds are no longer directly under those shown for the upper ML_4 group, the sign of the $\delta \rightarrow \delta^*$ CD band is given by the signs of the sectors in which they fall. Two important points are (1) the presence of chains of atoms connecting upper and lower L atoms and the positions of those chains are irrelevant, since the chirality at the chromophore is dominated by the eight coordinated atoms, and (2) a twist angle of χ and one of $\chi - 90°$ have the same effect on the sign of the CD.

The $Mo_2Cl_4(DIOP)_2$ molecules studied here are the first ones of the general class represented in Figure 1b to have χ between 45° and 90°. Figure 8 also shows axial views of the two isomers of $Mo_2Cl_4[(R,R)\text{-DIOP}]_2$. According to the sector diagram the Δ and Λ forms of such a molecule should show – and + CD bands, respectively, for the $\delta \rightarrow \delta^*$ transition. Since a solution of $Mo_2Cl_4[(R,R)\text{-DIOP}]_2$ contains 1.7 times as many P molecules as S molecules, the rule predicts that the solution should show a net positive CD band for the $\delta \rightarrow \delta^*$ transition and, for the reason mentioned earlier, a negative CD band for the transition at 490 nm. This is what is observed, as Figure 4 shows.

Concluding Remarks. The work reported here has benefited from two pleasant surprises, namely that the compound (which contains two fused eight-membered rings) could actually be prepared and that it displayed a mean torsion angle in the 45° $< \chi <$ 90° range. Both of these features may be attributed to the conformational restraints imposed by shape and rigidity of the incorporated five-membered dioxo ring. This helps to overcome the entropic factor disfavoring the closure of such a large ring and also imposes restraints that lead to the large torsion angles about the Mo–Mo bond. Still another surprise was that this molecule was not only able to exist in two conformationally isomeric forms in solution, but that in the crystal they were able to coexist and share the same set of sites, just as had much simpler $\beta\text{-}M_2X_4(LL)_2$ molecules where there was no chirality inherent in the ligands. All of these features taken together have enabled us to acquire information about $\beta\text{-}M_2X_4(LL)_2$ molecules that had heretofore been inaccessible.

The results obtained here also suggest some further studies that we shall attempt to carry out. One of the most interesting will be to examine the NMR spectra of other $\beta\text{-}M_2X_4(diphos)_2$ in solution to see if they, too, exist as mixtures of two isomers. In all previous discussions it has been tacitly assumed that for a compound like $Mo_2Cl_4[(S,S)\text{-dppb}]_2$ where only one isomer occurred in the crystal,[4] only this one isomer would be present in solution. It is now clear that this need not be true. From what we have learned in the present study, it seems certain that should a second isomer be present, we shall be able to detect it by NMR. It is also now of interest, and clearly feasible, to see if other $\beta\text{-}Mo_2X_4(diphos)_2$ molecules that do show two isomers in the crystal will continue to do so in solution, and also to determine the ratio. Once ratios of isomers for the resolved chiral compounds are known, it may be possible to obtain quantitative relationships between the rotational strengths of CD bands and the internal twist angles.

Acknowledgment. We thank the National Science Foundation for support.

Supplementary Material Available: Complete tables of anisotropic thermal parameters, bond distances, bond angles, torsional angles for the central portion of the molecule, and distances and angles of selected protons of $\Delta\text{-}Mo_2Cl_4[(R,R)\text{-DIOP}]_2$ and $\Lambda\text{-}Mo_2Cl_4[(R,R)\text{-DIOP}]_2$ (16 pages); listings of observed and calculated structure factors (32 pages). Ordering information is given on any current masthead page.

Electron-Transfer Self-Exchange Kinetics of Cytochrome b_5

Dabney White Dixon,*,† Xiaole Hong,† Scott E. Woehler,† A. Grant Mauk,*,‡ and Bhavini P. Sishta‡

Contribution from the Department of Chemistry and Laboratory for Microbial and Biochemical Sciences, Georgia State University, Atlanta, Georgia 30303, and the Department of Biochemistry, University of British Columbia, Vancouver, British Columbia V6T 1W5, Canada.
Received December 12, 1988. Revised Manuscript Received September 13, 1989

Abstract: The electron-transfer self-exchange rate constant of trypsin-solubilized bovine liver microsomal cytochrome b_5 has been measured as a function of temperature and ionic strength. Calculations based on ^1H NMR spectra and using the inversion-recovery method determined this rate constant to be 2.6×10^3 M^{-1} s^{-1} [pH 7.0, μ = 0.1 M (sodium phosphate), 25 °C] with $\Delta H^* = 5.5$ kcal mol^{-1} and $\Delta S^* = -23$ eu (μ = 0.1–0.3 M). This rate constant increases with ionic strength, reaching a value of 4.5×10^4 M^{-1} s^{-1} at μ = 1.5 M. Analysis of the data in terms of Marcus theory gives a reorganization energy, λ, for self-exchange in the range 0.9–1.3 eV mol^{-1}. The components of the dipole moments through the exposed heme edge of the reduced and oxidized protein are estimated to be −280 and −250 D, respectively.

Metalloprotein electron-transfer reactions are fundamental phenomena that are characteristic of biological processes such as photosynthesis, oxidative phosphorylation, xenobiotic detoxification, and the catalytic cycles of several enzymes.[1] The rate of electron transfer between metalloproteins is a function of several factors including the thermodynamic driving force, distance between the donor and acceptor centers, reorganization energy of

† Georgia State University.
‡ University of British Columbia.

(1) (a) Michel-Beyerle, M. E., Ed. *Antennas and Reactions Centers of Photosynthetic Bacteria*; Springer-Verlag: New York, 1985. (b) Hatefi, Y. *Annu. Rev. Biochem.* **1985**, *54*, 1015. (c) Blumberg, W. E. *Q. Rev. Biophys.* **1978**, *4*, 481. (d) Dreyer, J. L. *Experientia* **1984**, *40*, 653. (e) Pettigrew, G. W.; Moore, G. R. *Cytochromes c. Biological Aspects*; Springer-Verlag: New York, 1987; p 29.

0002-7863/90/1512-1082$02.50/0